

GT2023–102024

AERO-ENGINES AI - A MACHINE-LEARNING APP FOR AIRCRAFT ENGINE CONCEPTS ASSESSMENT

Michael T. Tong

National Aeronautics and Space Administration
John H. Glenn Research Center
Cleveland, Ohio 44135

ABSTRACT

Effective deployment of machine-learning (ML) models could drive a high level of efficiency in aircraft engine conceptual design. *Aero-Engines AI* is a user-friendly app that has been created to deploy trained machine-learning (ML) models to assess aircraft engine concepts. It was created using *tkinter*, a GUI (graphical user interface) module that is built into the standard Python library. Employing *tkinter* greatly facilitates the sharing of ML application as an executable file which can be run on Windows machines (without the need to have Python or any library installed). The app gets user input for a turbofan design, preprocesses the input data, and deploys trained ML models to predict turbofan thrust specific fuel consumption (TSFC), engine weight, core size, and turbomachinery stage-counts. The ML predictive models were built by employing supervised deep-learning and K-nearest neighbor regression algorithms to study patterns in an existing open-source database of production and research turbofan engines. They were trained, cross-validated, and tested in Keras, an open-source neural networks API (application programming interface) written in Python, with TensorFlow (Google open-source artificial intelligence library) serving as the backend engine. The smooth deployment of these ML models using the app shows that *Aero-Engines AI* is an easy-to-use and a time-saving tool for aircraft engine design-space exploration during the conceptual design stage. Current version of the app focuses on the performance prediction of conventional turbofans. However, the scope of the app can easily be expanded to include other engine types (such as turbohaft and hybrid-electric systems) after their ML models are developed. Overall, the use of a machine-learning app for aircraft engine concept assessment represents a promising area of development in aircraft engine conceptual design.

Keywords: aircraft engine, machine learning, tkinter, Python, TensorFlow

INTRODUCTION

More and more organizations are adopting a data-driven approach to decision-making. With the vast amounts of data

collected and tracked in recent times, machine-learning (ML) applications are gaining popularity across multiple industries. The aircraft engine industry has amassed and stored significant quantities of data over the years. These big data sets, sourced from multiple origins such as the database of currently manufactured engines, ongoing development projects, previously completed development projects, and unmanufactured designs, hold tremendous potential as a knowledge asset for future engine projects.

Designing an aircraft engine is a complex, interdisciplinary process that requires significant time and effort. Engine designers encounter a formidable challenge during the conceptual design phase - how to rapidly evaluate the performance of a specific engine design given the aircraft's mission requirements and various design parameters. The number of potential engine configurations could be vast, requiring designers to rely on system analysis and simulation to estimate performance. Consequently, designers must conduct a comprehensive propulsion system study for each possible configuration, which can be time-consuming, particularly when dealing with a large design space.

By leveraging the power of machine learning (ML) algorithms to learn from the existing engine data sets, it is possible to develop ML models that can quickly and accurately assess new aircraft engine concepts, providing valuable insights and reducing the time and resources required for the engine concept assessment process. A ML model can identify patterns and trends that may not be immediately apparent to human analysts, leading to more informed decision-making and ultimately resulting in the development of better aircraft engine concepts. The ability to assess new engine concepts quickly and accurately can be a competitive advantage in aircraft engine development.

Previously, the author focused on training/developing the ML models that allow for quick estimation of engine TSFC, system weight, and core size during the conceptual design

phase. The development process and methodology for these models are described in [1, 2, 3]. Additional ML models were developed for the turbomachinery stage count prediction since then, using the same methodology. This paper zeros in on the deployment of these trained ML models to assess aircraft engine concepts, via an app. The development process of the app, *Aero-Engines AI*, is described in this paper.

While the development of ML models is essential for their applications, the models would only be of value if they are actively deployed in a production environment where they can be used to solve practical problems. Thus, effective ML model deployment is just as important as ML model development. ML model deployment involves integrating trained ML models, developed in a R&D environment, into a production environment. It is a critical step that must be done so an organization can use the models to solve problems. Seamless deployment of trained ML models into production is essential for putting the models to practical use.

Aero-Engines AI, a Windows app, has been created to deploy the trained ML models for aircraft engine concepts assessment. It was created using *tkinter*, a GUI module that is built into the standard Python library. Employing *tkinter* greatly facilitates the sharing of ML application as an executable file which can be run on Windows machines (without the need to have Python or any library installed). MS Windows platform was chosen for the deployment to reduce complexity and for ease of access. The structure of the app is shown in Figure 1.

The app is user-friendly. It is simple to learn, easy to navigate, and its use is intuitive enough that it does not require an instruction manual. The development process of *Aero-Engines AI* consists of five steps:

- Engine data collection, augmentation, and preparation
- ML models training
- ML models testing and evaluation
- App design for ML models deployment
- Monitoring and updating

ENGINE DATA COLLECTION, AUGMENTATION, AND PREPARATION

• Engine data collection
 Current version of the app has only turbofan assessment capability (will be expanded to include other engine types such as turboshaft, hybrid-turbofan, etc., in the future versions). The basic engine architecture is an axial-compressor turbofan. The engine database consists of 145 manufactured (commercial) engines [4 to 10] and 39 engines that were studied previously in various NASA aeronautics projects. These commercial engines capture over half-a-century of engine technology improvements and lessons-learned, which would minimize the prediction uncertainties of the ML models. The NASA engine

data were the system-study results for various NASA aeronautics projects [11–16]. The engine database is shown in Appendix A.

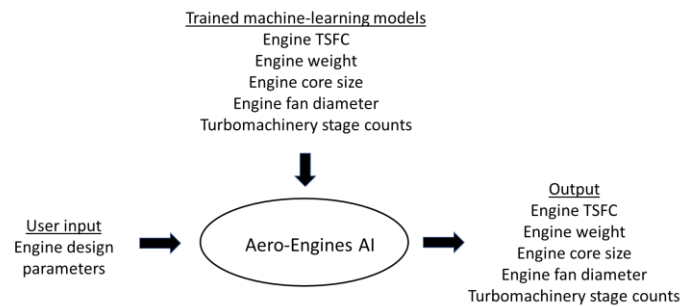


Figure 1 – Structure of *Aero-Engines AI* app

- Data augmentation
 Data augmentation is an important technique that is commonly used in ML to improve the performance and generalizability of a training model. The process entails creating additional data points from the existing training data by applying various transformations and modifications to the data. Data augmentation increases the diversity and quantity of training data, improving the model's performance for its task, and making it more adaptable to changes in the data. For this study, the data augmentation was performed by scaling up the current engines by 10%. For example, the sea-level static (SLS) engine thrust and weight were increased by 10%, while keeping the other operating parameters such as bypass ratio (BPR), overall pressure ratio (OPR), Mach No., altitude, and TSFC unchanged, as shown below:

| BPR | OPR | SLS Thrust (lbs) | Mach | Alt. (ft) | TSFC (lb/hr/lb) | Weight (lbs) |
|------|-------|------------------|------|-----------|-----------------|--------------|
| 8.44 | 38.37 | 79377 | 0.85 | 35000 | .5526 | 18949 |
| 8.44 | 38.37 | 87315 | 0.85 | 35000 | .5526 | 20844 |

With the data augmentation, the size of the database becomes:

| Turbofan type | No. of engines |
|----------------------|----------------|
| 2-spool direct-drive | 273 |
| 2-spool geared | 89 |
| 3-spool direct-drive | 50 |

- Dataset preparation
 The next step was to prepare the data that would be used to train the ML models. It involved cleaning and preprocessing the data to remove errors or inconsistencies and organizing the data into a format that could be used for the training. The engine dataset was normalized and shuffled randomly (using pseudo-random number generator) and divided into two datasets: the training set and the testing set. The training set was used to train, cross-validate, and build predictive models. The testing set consisted of the remaining engines that were unseen by the training models and was

retained for the final evaluation of the predictive analytics. The dataset preparation is described in detail in [1, 2, and 3].

ML MODELS TRAINING

Once the data was ready, the next step was to select the appropriate algorithms that would be used to train the ML models. This can involve choosing from a variety of machine learning algorithms and tuning the parameters and hyperparameters of the models to optimize their performance on the specific problem or task.

As reported in [1, 2, 3], the ML models for TSFC, engine weight, and core size predictions were constructed using supervised deep-learning and K-nearest neighbor algorithms [17], which analyzed patterns in an open-source database of research and production turbofan engines. Additional ML models were developed since then for the turbomachinery stage count prediction, using K-nearest neighbor regression algorithm. These models were trained, cross-validated, and tested using Keras, an open-source neural networks API written in Python, with TensorFlow as the backend engine. These models were trained and deployed in Keras [18], an open-source neural networks API written in Python, with TensorFlow [19] serving as the backend engine. Keras provided the building blocks for developing the deep-learning models, and TensorFlow handled the tensor computations and manipulations.

Depending on the ML model, either *L2* or *Dropout* regularization technique (where neuron outputs are dropped out randomly) [20 and 21] was applied to prevent the DNN from overfitting the training data. A grid-search routine was used to determine the regularization parameter, dropout rate, number of epochs, batch size, and the number of ‘neurons’ in the hidden layers that give the lowest training error. The Adam optimization algorithm [22] was used to update the network weights during each epoch.

Totally, nine ML models were trained for engine *TSFC*, *weight*, *core size* (last stage HPC blade height), fan diameter, and *turbomachinery stage count* predictions, respectively. The training and cross validation of these ML models are described in detail in [1, 2, and 3].

ML MODELS TESTING

After the ML models were trained, the next step was to test and evaluate their performances. The trained ML models were evaluated using a separate set of data, the testing dataset (that was unseen by the training models). The testing procedures of these ML models are described in detail in [1, 2, 3]. The results showed that these ML models are an effective tool for predicting engine TSFC, engine weight, core size, and turbomachinery stage counts. Their performances were determined, in terms of the means and standard deviations:

| ML model | Mean accuracy | Uncertainty 95% confidence interval (2 standard deviations) |
|-----------------|---------------|---|
| TSFC | 98% | 4% |
| Weight | 95% | 5% |
| Core size | 98% | 4% |
| Fan diameter | 98% | 5% |
| LPC stage count | 98% | 14% (or 1 stage [*]) |
| HPC stage count | 98% | 8% (or 1 stage [*]) |
| HPT stage count | 96% | 39% (or 1 stage [*]) |
| LPT stage count | 98% | 18% (or 1 stage [*]) |
| IPT stage count | 90% | 44% (or 1 stage [*]) |

Notes: ^{*}based on the current database
1-stage fan is assumed for all the engines

APP DESIGN for ML MODELS DEPLOYMENT

After the ML models were developed, trained, and tested, they were integrated into the user-friendly app, *Aero-Engines AI*, that allows for the easy and intuitive assessment of engine concepts. *Aero-Engines AI* is a Windows app that deploys trained ML models to assess aircraft engine concepts. The app was created using *tkinter* [23], a GUI (graphical user interface) module that is built into the standard Python library. And *pyinstaller* [24], a Python package, was used to convert the python scripts into an executable file that can be run on Windows machines. The conversion greatly facilitates the sharing of ML applications with other Windows users (who do not need to have Python, or any library installed in their computers).

The app design aimed to provide a user-friendly experience with a simple point-and-click feature. The input page consists of three elements:

- a drop-down menu to select options
- data entry fields
- a ‘PREDICT’ button to run the app

These three elements are shown in Figure 2.

The drop-down menu allows users to select different options for engine architectures, configurations, and timeframe. When a user selects a tab, the drop-down menu will display the options that are associated with that tab. Based on the user's selection, the app would use the trained ML models to analyze relevant data and make predictions on engine performance, in terms of engine TSFC, weight, core size, and turbomachinery stage counts. The drop-down menu consists of the following tabs:

Engine type – current version of the app only has the conventional turbofans option. Turbohaft and hybrid-electric

turbofan are being considered for the future app versions. The engine-type tab is shown in Figure 3.

Drive system – offers two options: direct-drive or geared. This tab is shown in Figure 4.

Engine configuration – offers two options: 2-spool or 3-spool design. This tab is shown in Figure 5.

Engine timeframe – engine certified year. Users can pick a calendar year or NASA timeframe (N+1, N+2, etc.). This tab is shown in Figure 6.

Single engine or Multiple engine designs – offers two options: single engine design or multiple-engine designs analyses. This tab is shown in Figure 7. If “multiple engine designs” is selected, the user inputs for bypass ratio, overall pressure ratio, and engine thrust would be in ranges, as shown in Figure 8.

The data entry fields are provided for the users to input the engine design parameters. The default entries for the Mach

number and cruise altitude are provided (0.8 and 35000 feet, respectively), as shown in Figure 2. The users can override these numbers.

App Execution - to run the app, one simply clicks the ‘PREDICT’ button.

Input Changes – users can return to the input page and modify the inputs by clicking the ‘BACK’ button on the output page. This button is shown in Figure 9.

Example Problems -

- Single engine design: -
input parameters are shown in Figure 7,
outputs are shown in Figure 9.
- Multiple engine designs: -
input parameters are shown in Figure 8,
output spreadsheet is shown in Figure 10

Aero-Engines AI
A machine-learning app for aero-engine concepts assessment

Turbofan | Direct-Drive | 2-Spool | Engine Timeframe | Single Engine Design

Drop-down menu

Engine design parameters input:

Sea level static engine bypass ratio (BPR, ≥ 1):

Sea level static overall pressure ratio (OPR, ≥ 16):

Sea level static thrust (lbf):

Cruise Mach No. ($0.7 \leq M \leq 0.9$): 0.8

Cruise altitude (feet, $30000 \leq \text{alt} \leq 45000$): 35000

Fan diameter known? Yes No

PREDICT App execution button

Figure 2 – User input page for single-engine design

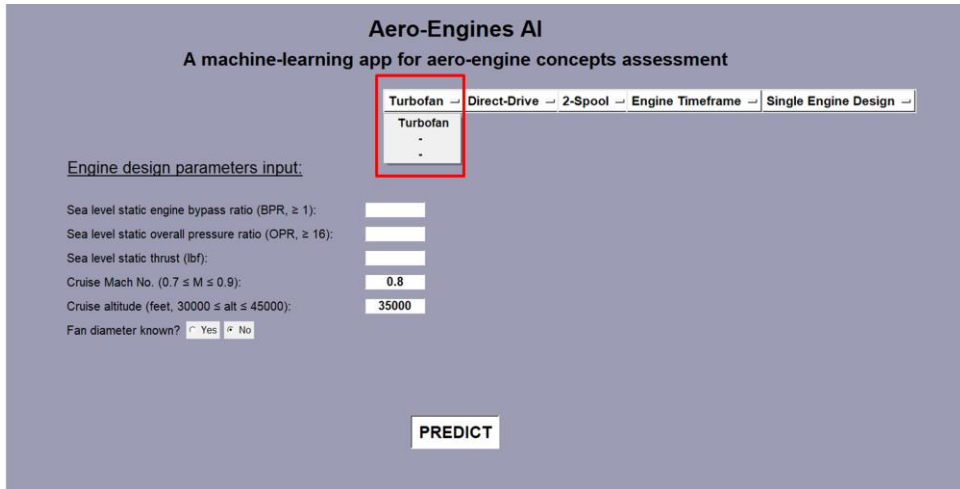


Figure 3 – Engine type option

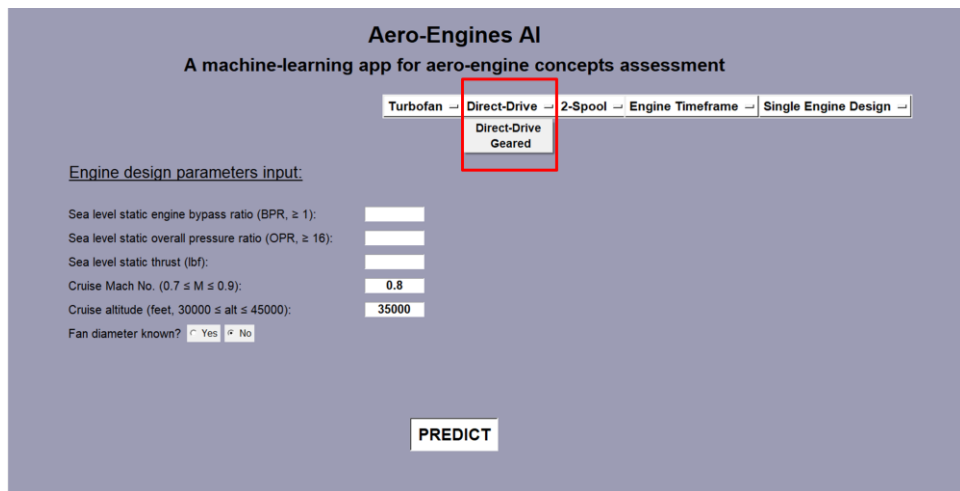


Figure 4 – Direct-drive or geared turbofan option

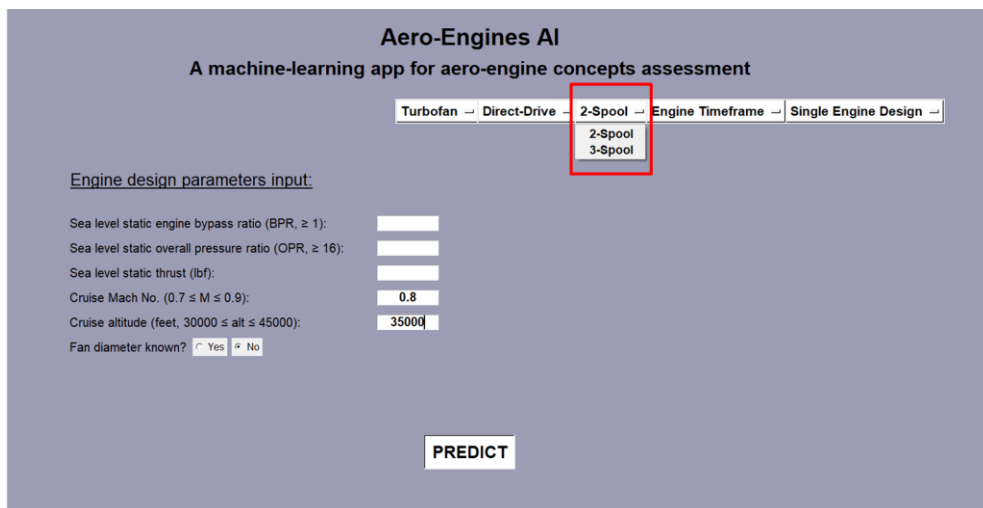


Figure 5 – Engine configuration options

Aero-Engines AI
A machine-learning app for aero-engine concepts assessment

Turbofan Direct-Drive 2-Spool Engine Timeframe Single Engine Design

Engine design parameters input:

Sea level static engine bypass ratio (BPR, ≥ 1):

Sea level static overall pressure ratio (OPR, ≥ 16):

Sea level static thrust (lbf):

Cruise Mach No. ($0.7 \leq M \leq 0.9$):

Cruise altitude (feet, $30000 \leq \text{alt} \leq 45000$):

Fan diameter known? Yes No

PREDICT

Figure 6 – Engine timeframe option

Aero-Engines AI
A machine-learning app for aero-engine concepts assessment

Turbofan Direct-Drive 2-Spool Year 2020 Single Engine Design

Engine design parameters input:

Sea level static engine bypass ratio (BPR, ≥ 1):

Sea level static overall pressure ratio (OPR, ≥ 16):

Sea level static thrust (lbf):

Cruise Mach No. ($0.7 \leq M \leq 0.9$):

Cruise altitude (feet, $30000 \leq \text{alt} \leq 45000$):

Fan diameter known? Yes No

PREDICT

Figure 7 – Single-engine or multiple-engine design option

Aero-Engines AI
A machine-learning app for aero-engine concepts assessment

Turbofan Geared 2-Spool Year 2035 Multiple Engine Designs

Engine design parameters input:

Sea level static engine bypass ratio range (BPR): (min, ≥ 1) (max, <36) (max. no. of step)

Sea level static overall pressure ratio range (OPR): (min, ≥ 16) (max, <55) (max. no. of step)

Sea level static thrust range (lbf): (min) (max) (max. no. of step)

Cruise Mach No. ($0.7 \leq M \leq 0.9$):

Cruise altitude (feet, $30000 \leq \text{alt} \leq 45000$):

PREDICT

Figure 8 – Input page for multiple-engine designs

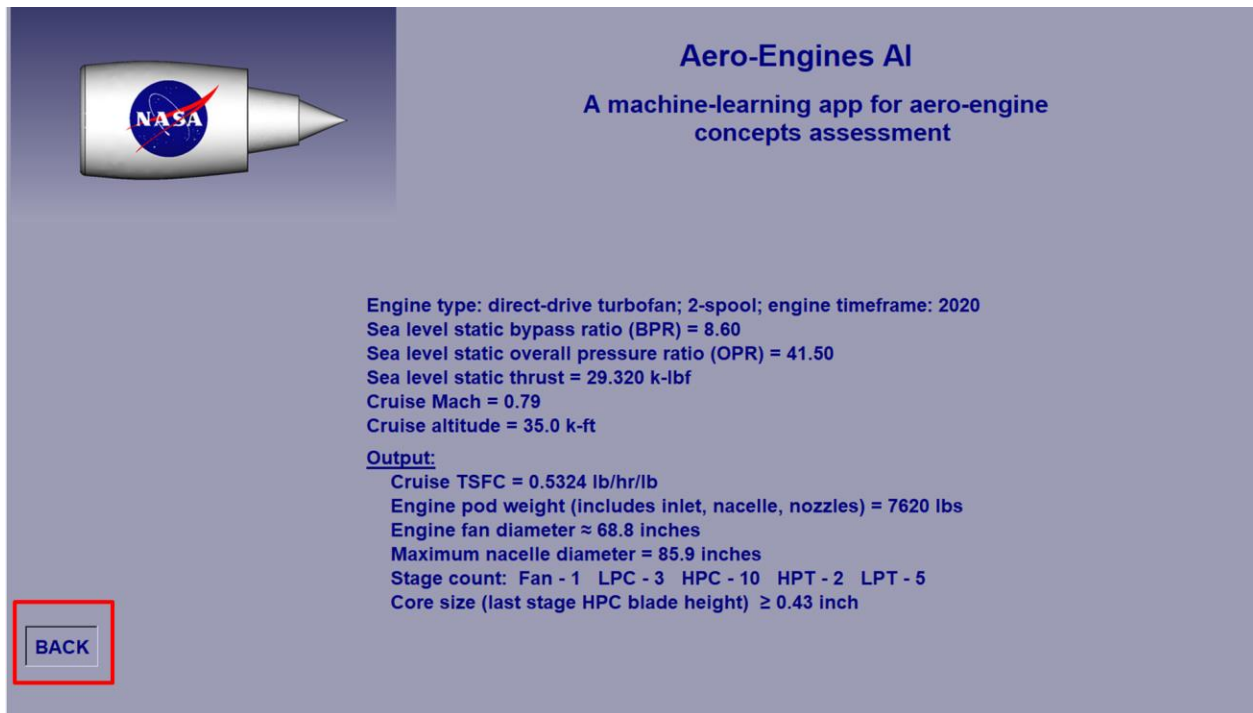


Figure 9 – Example output of a single-engine design

MONITORING AND UPDATING

Monitoring and updates are important aspects of ML app development, as they help ensure that the app continues to perform well and provide accurate predictions or recommendations over time. To ensure optimal performance of the current ML models, it's crucial to keep track of the changing engine data and its effect on their overall functionality. While the commercial engine data in the current database remain static, the NASA engine data are obtained through research on aeronautics studies for three generations of aircraft - near, mid, and far term. Each generation has associated goals for reductions in noise, emissions, fuel burn, and field length relative to present-day aircrafts. These aircraft generations are labeled as 'N+1', 'N+2', and 'N+3', respectively. The research for 'N+2' and 'N+3' is aimed at enabling new vehicle configurations that meet NASA's ambitious technology objectives. As the NASA engine data could be revised over time, the ML models must be updated periodically to consider the impact of such updates.

SUMMARY

Aero-Engines AI, a user-friendly Windows app, has been created using *tkinter*, a GUI module that is built into the standard Python library. This app is designed to deploy trained ML models to assess various aircraft engine concepts. These ML models were trained, cross-validated, and tested in Keras,

an open-source neural networks API written in Python, with TensorFlow serving as the backend engine. The assessment results are presented in terms of engine TSFC, weight, core size, and turbomachinery stage counts. The seamless deployment of these ML models through the app demonstrates that *Aero-Engines AI* is an efficient and easy-to-use tool for exploring the design space of aircraft engines during the conceptual design stage. The current version of the app focuses on predicting the performance of conventional turbofans. However, after the development of their ML models, the app's scope can be easily expanded to include other engine types, such as turboshaft and hybrid-electric systems.

The success of the ML application will depend on the quality and quantity of data available for training, as well as the deployment of the ML model itself. Careful consideration of these factors is crucial to ensure the optimal performance of the ML system. Overall, the use of a machine-learning app for aircraft engine concept assessment represents a promising area of development in aircraft engine conceptual design.

ACKNOWLEDGMENT

The work presented in this paper was supported by the NASA Advanced Air Transport Technology Project of the Advanced Air Vehicles Program.

engine_output.xlsx Search (Alt+Q) Michael Tong

File Home Insert Page Layout Formulas Data Review View Help Power Pivot

A1 SLS OPR

| | A | B | C | D | E | F | G | H | I | J | K | L | M | N | O | P | Q | R | S | T |
|----|---------|---------|--------------------|-------------|------------------|------------|-----------|------------------|---------------|------------------------|-----------------------|-----------------|-----------------------------|-------------|-------------|-------------|-------------|-------------|-------------|---|
| 1 | SLS OPR | SLS BPR | SLS Thrust, k-lbfs | Cruise Mach | Cruise Alt, k-ft | Drive Type | No. Spool | Engine Timeframe | Fan dia, inch | Max. nacelle dia, inch | Cruise TSFC, lb/hr/lb | Pod Weight, lbs | HPC last-stg blade-ht, inch | # fan stage | # LPC stage | # HPC stage | # HPT stage | # IPT stage | # LPT stage | |
| 2 | 36 | 11 | 26 | 0.8 | 43 | geared | 2-spool | 2035 | 71.36 | 87.48 | 0.5374 | 6631 | ≥ 0.43 inch | 1 | 3 | 9 | 2 | | 3 | |
| 3 | 36 | 11 | 27 | 0.8 | 43 | geared | 2-spool | 2035 | 72.74 | 89.17 | 0.5418 | 6859 | ≥ 0.43 inch | 1 | 3 | 9 | 2 | | 3 | |
| 4 | 36 | 11 | 28 | 0.8 | 43 | geared | 2-spool | 2035 | 74.29 | 91.08 | 0.5442 | 7118 | ≥ 0.43 inch | 1 | 3 | 9 | 2 | | 3 | |
| 5 | 36 | 12 | 26 | 0.8 | 43 | geared | 2-spool | 2035 | 73.05 | 89.56 | 0.5320 | 6760 | ≥ 0.43 inch | 1 | 3 | 9 | 2 | | 3 | |
| 6 | 36 | 12 | 27 | 0.8 | 43 | geared | 2-spool | 2035 | 74.58 | 91.43 | 0.5364 | 7020 | ≥ 0.43 inch | 1 | 3 | 9 | 2 | | 3 | |
| 7 | 36 | 12 | 28 | 0.8 | 43 | geared | 2-spool | 2035 | 76.19 | 93.41 | 0.5400 | 7309 | ≥ 0.43 inch | 1 | 3 | 9 | 2 | | 3 | |
| 8 | 36 | 13 | 26 | 0.8 | 43 | geared | 2-spool | 2035 | 74.79 | 91.70 | 0.5272 | 6907 | ≥ 0.43 inch | 1 | 3 | 9 | 2 | | 3 | |
| 9 | 36 | 13 | 27 | 0.8 | 43 | geared | 2-spool | 2035 | 76.53 | 93.82 | 0.5317 | 7202 | ≥ 0.43 inch | 1 | 3 | 9 | 2 | | 3 | |
| 10 | 36 | 13 | 28 | 0.8 | 43 | geared | 2-spool | 2035 | 78.37 | 96.08 | 0.5356 | 7500 | ≥ 0.43 inch | 1 | 3 | 9 | 2 | | 3 | |
| 11 | 36 | 14 | 26 | 0.8 | 43 | geared | 2-spool | 2035 | 75.29 | 92.31 | 0.5231 | 6874 | ≥ 0.43 inch | 1 | 3 | 9 | 2 | | 3 | |
| 12 | 36 | 14 | 27 | 0.8 | 43 | geared | 2-spool | 2035 | 76.92 | 94.30 | 0.5273 | 7160 | ≥ 0.43 inch | 1 | 3 | 9 | 2 | | 3 | |
| 13 | 36 | 14 | 28 | 0.8 | 43 | geared | 2-spool | 2035 | 78.64 | 96.42 | 0.5313 | 7451 | ≥ 0.43 inch | 1 | 3 | 9 | 2 | | 3 | |
| 14 | 36 | 15 | 26 | 0.8 | 43 | geared | 2-spool | 2035 | 76.60 | 93.91 | 0.5195 | 6947 | ≥ 0.43 inch | 1 | 4 | 9 | 2 | | 3 | |
| 15 | 36 | 15 | 27 | 0.8 | 43 | geared | 2-spool | 2035 | 78.26 | 95.95 | 0.5235 | 7234 | ≥ 0.43 inch | 1 | 4 | 9 | 2 | | 3 | |
| 16 | 36 | 15 | 28 | 0.8 | 43 | geared | 2-spool | 2035 | 80.02 | 98.11 | 0.5275 | 7529 | ≥ 0.43 inch | 1 | 4 | 9 | 2 | | 3 | |
| 17 | 37 | 11 | 26 | 0.8 | 43 | geared | 2-spool | 2035 | 71.40 | 87.53 | 0.5375 | 6640 | ≥ 0.43 inch | 1 | 3 | 9 | 2 | | 3 | |
| 18 | 37 | 11 | 27 | 0.8 | 43 | geared | 2-spool | 2035 | 72.79 | 89.24 | 0.5417 | 6863 | ≥ 0.43 inch | 1 | 3 | 9 | 2 | | 3 | |
| 19 | 37 | 11 | 28 | 0.8 | 43 | geared | 2-spool | 2035 | 74.24 | 91.02 | 0.5424 | 7102 | ≥ 0.43 inch | 1 | 3 | 9 | 2 | | 3 | |
| 20 | 37 | 12 | 26 | 0.8 | 43 | geared | 2-spool | 2035 | 73.34 | 89.92 | 0.5322 | 6795 | ≥ 0.43 inch | 1 | 3 | 9 | 2 | | 3 | |
| 21 | 37 | 12 | 27 | 0.8 | 43 | geared | 2-spool | 2035 | 74.87 | 91.79 | 0.5363 | 7051 | ≥ 0.43 inch | 1 | 3 | 9 | 2 | | 3 | |
| 22 | 37 | 12 | 28 | 0.8 | 43 | geared | 2-spool | 2035 | 76.48 | 93.76 | 0.5384 | 7337 | ≥ 0.43 inch | 1 | 3 | 9 | 2 | | 3 | |
| 23 | 37 | 13 | 26 | 0.8 | 43 | geared | 2-spool | 2035 | 75.89 | 93.04 | 0.5275 | 7035 | ≥ 0.43 inch | 1 | 3 | 9 | 2 | | 3 | |
| 24 | 37 | 13 | 27 | 0.8 | 43 | geared | 2-spool | 2035 | 77.62 | 95.16 | 0.5317 | 7327 | ≥ 0.43 inch | 1 | 3 | 9 | 2 | | 3 | |
| 25 | 37 | 13 | 28 | 0.8 | 43 | geared | 2-spool | 2035 | 79.21 | 97.11 | 0.5346 | 7588 | ≥ 0.43 inch | 1 | 3 | 9 | 2 | | 3 | |
| 26 | 37 | 14 | 26 | 0.8 | 43 | geared | 2-spool | 2035 | 76.00 | 93.18 | 0.5233 | 6950 | ≥ 0.43 inch | 1 | 4 | 9 | 2 | | 3 | |
| 27 | 37 | 14 | 27 | 0.8 | 43 | geared | 2-spool | 2035 | 77.65 | 95.20 | 0.5275 | 7238 | ≥ 0.43 inch | 1 | 4 | 9 | 2 | | 3 | |
| 28 | 37 | 14 | 28 | 0.8 | 43 | geared | 2-spool | 2035 | 79.39 | 97.33 | 0.5311 | 7525 | ≥ 0.43 inch | 1 | 4 | 9 | 2 | | 3 | |
| 29 | 37 | 15 | 26 | 0.8 | 43 | geared | 2-spool | 2035 | 76.86 | 94.23 | 0.5197 | 6962 | ≥ 0.43 inch | 1 | 4 | 9 | 2 | | 3 | |
| 30 | 37 | 15 | 27 | 0.8 | 43 | geared | 2-spool | 2035 | 78.47 | 96.20 | 0.5236 | 7246 | ≥ 0.43 inch | 1 | 4 | 9 | 2 | | 3 | |
| 31 | 37 | 15 | 28 | 0.8 | 43 | geared | 2-spool | 2035 | 80.17 | 98.29 | 0.5274 | 7530 | ≥ 0.43 inch | 1 | 4 | 9 | 2 | | 3 | |
| 32 | 38 | 11 | 26 | 0.8 | 43 | geared | 2-spool | 2035 | 71.46 | 87.61 | 0.5372 | 6658 | ≥ 0.43 inch | 1 | 3 | 9 | 2 | | 3 | |
| 33 | 38 | 11 | 27 | 0.8 | 43 | geared | 2-spool | 2035 | 72.88 | 89.35 | 0.5398 | 6874 | ≥ 0.43 inch | 1 | 3 | 9 | 2 | | 3 | |
| 34 | 38 | 11 | 28 | 0.8 | 43 | geared | 2-spool | 2035 | 74.36 | 91.17 | 0.5403 | 7112 | ≥ 0.43 inch | 1 | 3 | 9 | 2 | | 3 | |
| 35 | 38 | 12 | 26 | 0.8 | 43 | geared | 2-spool | 2035 | 73.67 | 90.32 | 0.5324 | 6828 | ≥ 0.43 inch | 1 | 3 | 9 | 2 | | 3 | |
| 36 | 38 | 12 | 27 | 0.8 | 43 | geared | 2-spool | 2035 | 75.20 | 92.19 | 0.5358 | 7079 | ≥ 0.43 inch | 1 | 3 | 9 | 2 | | 3 | |
| 37 | 38 | 12 | 28 | 0.8 | 43 | geared | 2-spool | 2035 | 76.80 | 94.16 | 0.5363 | 7358 | ≥ 0.43 inch | 1 | 3 | 9 | 2 | | 3 | |
| 38 | 38 | 13 | 26 | 0.8 | 43 | geared | 2-spool | 2035 | 76.45 | 93.72 | 0.5278 | 7088 | ≥ 0.43 inch | 1 | 4 | 9 | 2 | | 3 | |
| 39 | 38 | 13 | 27 | 0.8 | 43 | geared | 2-spool | 2035 | 77.98 | 95.61 | 0.5317 | 7358 | ≥ 0.43 inch | 1 | 4 | 9 | 2 | | 3 | |
| 40 | 38 | 13 | 28 | 0.8 | 43 | geared | 2-spool | 2035 | 79.46 | 97.41 | 0.5325 | 7601 | ≥ 0.43 inch | 1 | 4 | 9 | 2 | | 3 | |
| 41 | 38 | 14 | 26 | 0.8 | 43 | geared | 2-spool | 2035 | 77.00 | 94.41 | 0.5236 | 7063 | ≥ 0.43 inch | 1 | 4 | 9 | 2 | | 3 | |
| 42 | 38 | 14 | 27 | 0.8 | 43 | geared | 2-spool | 2035 | 78.72 | 96.52 | 0.5275 | 7359 | ≥ 0.43 inch | 1 | 4 | 9 | 2 | | 3 | |
| 43 | 38 | 14 | 28 | 0.8 | 43 | geared | 2-spool | 2035 | 80.40 | 98.58 | 0.5289 | 7629 | ≥ 0.43 inch | 1 | 4 | 9 | 2 | | 3 | |
| 44 | 38 | 15 | 26 | 0.8 | 43 | geared | 2-spool | 2035 | 77.64 | 95.19 | 0.5198 | 7045 | ≥ 0.43 inch | 1 | 4 | 9 | 2 | | 3 | |
| 45 | 38 | 15 | 27 | 0.8 | 43 | geared | 2-spool | 2035 | 79.27 | 97.18 | 0.5237 | 7332 | ≥ 0.43 inch | 1 | 4 | 9 | 2 | | 3 | |
| 46 | 38 | 15 | 28 | 0.8 | 43 | geared | 2-spool | 2035 | 80.88 | 99.16 | 0.5256 | 7598 | ≥ 0.43 inch | 1 | 4 | 9 | 2 | | 3 | |
| 47 | | | | | | | | | | | | | | | | | | | | |
| 48 | | | | | | | | | | | | | | | | | | | | |

Sheet1

Ready

Figure 10 - Example spreadsheet output of multiple-engine designs

REFERENCES

- [1] Tong, M. T., “Using Machine Learning to Predict Core Sizes of High-Efficiency Turbofan Engines,” GTP-19-1338, ASME Journal of Engineering for Gas Turbines and Power, Volume 141, Issue 11, November 2019.
- [2] Tong, M. T., “Machine Learning-Based Predictive Analytics for Aircraft Engine Conceptual Design,” NASA TM-20205007448, October 2020.
- [3] Tong, M. T., “A Machine-Learning Approach to Assess Aircraft Engine System Performance,” GT-2020-14661, Proceedings of ASME Turbo Expo 2020, September 21–25, 2020 (virtual conference).
- [4] Daly, M., 2018, “Jane’s Aero-Engine,” IHS, London, UK.
- [5] Meier, N., 2018, “Civil Turbojet/Turbofan Specifications,” accessed Aug. 8, 2018, <http://www.jet-engine.net/civtfspec.html>
- [6] GE Aviation, 2018, “GE Aviation,” GE Aviation, Evendale, OH, accessed Aug. 8, 2018, <https://www.geaviation.com/commercial>
- [7] Pratt and Whitney, 2018, “Commercial-Engines,” Pratt and Whitney, East Hartford, CT, accessed Aug. 8, 2018, <https://www.pw.utc.com/products-and-services/products/commercial-engines>
- [8] Rolls Royce, 2018, “Rolls Royce,” Rolls Royce, Derby, UK, accessed Aug. 8, 2018, <https://www.rolls-royce.com/products-and-services/civil-aerospace>
- [9] CFM International, 2018, “CFM International,” CFM International, Cincinnati, OH, accessed Aug. 8, 2018, <https://www.cfmaeroengines.com/>
- [10] International Civil Aviation Organization, 2018, “ICAO Aircraft Emissions Databank,” International Civil Aviation Organization, Montreal, Canada.
- [11] Guynn, M.D., Berton, J.J., Fisher, K.L., Haller, W.J., Tong, M., Thurman, D.R., “Engine Conceptual Study for an Advanced Single-Aisle Transport,” NASA TM-2009-215784, August 2009.
- [12] Guynn, M.D., Berton, J.J., Fisher, K.L., Haller, W.J., Tong, M., Thurman, D.R., “Analysis of Turbofan Design Options for an Advanced Single-Aisle Transport Aircraft,” AIAA 2009-6942, September 2009.
- [13] Guynn, M. D., Berton, J.J., Fisher, K.L., Haller, W.J., Tong, M., Thurman, D.R., “Refined Exploration of Turbofan Design Options for an Advanced Single-Aisle Transport,” NASA TM-2011-216883, January 2011.
- [14] Guynn, M.D., Berton, J.J., Tong, M.T., Haller, W.J., “Advanced Single-Aisle Transport Propulsion Design Options Revisited,” AIAA 2013-4330, August 2013.
- [15] Nickol, C.L. and Haller W.J., “Assessment of the Performance Potential of Advanced Subsonic Transport Concepts for NASA’s Environmentally Responsible Aviation Project,” AIAA 2016-1030, January 2016.
- [16] Collier, F., Thomas, R., Burley, C., Nickol, C., Lee, C.M., Tong, M., “Environmentally Responsible Aviation – Real Solutions for Environmental Challenges Facing Aviation,” 27th International Congress of the Aeronautical Sciences, September, 2010.
- [17] Geron, A., “Hands-On Machine Learning with Scikit-Learn and TensorFlow,” first edition, March 2017. Published by O’Reilly Media, Inc.
- [18] Chollet, François and others, “Keras.” accessed February 22, 2019, <https://keras.io/>
- [19] Google, “TensorFlow: Large-Scale Machine Learning on Heterogeneous Distributed Systems.” accessed February 20, 2019, <https://www.tensorflow.org/>
- [20] Ng, A., 2004 “Feature selection, L_1 vs. L_2 regularization, and rotational invariance,” Proceedings of the twenty-first international conference on Machine learning, July 4, 2004
- [21] Hinton, G.E., Krizhevsky, A., Srivastava, N., Sutskever, I., & Salakhutdinov, R., “Dropout: A simple Way to Prevent Neural Networks from Overfitting.” Journal of Machine Learning Research, 15, 1929-1958. June, 2014.
- [22] Kingma, D. P. and Ba, J., “Adam: A Method for Stochastic Optimization,” International Conference on Learning Representations, May 2015.
- [23] Van Rossum, G., et al., “The Python Library Reference, release 3.8.2,” Python Software Foundation, 2020.
- [24] Cortesi, D., “PyInstaller 5.7.0,” released on December 4, 2022, accessed December 19, 2022. <https://pypi.org/project/pyinstaller/>

Appendix A

Engine database

| <u>Org.</u> | <u>Engine Model</u> | <u>BPR (SLS)</u> | <u>OPR (SLS)</u> | <u>Thrust, lbs (SLS)</u> | <u>Cruise Mach</u> | <u>Cruise Alt. k ft.</u> | <u>Year certified</u> | <u>System Type</u> | <u>No. of Spools</u> | <u>Cruise TSFC lb/lbf.hr</u> | <u>Propulsion System Weight, lbs</u> |
|-------------|---------------------|------------------|------------------|------------------------------|------------------------|------------------------------|---------------------------|------------------------|--------------------------|----------------------------------|--|
| CFM Int'l | CFM56-2C1 | 6.0 | 23.50 | 22000 | 0.80 | 35 | 1979 | DD | 2 | 0.651 | 7199 |
| CFM Int'l | CFM56-3B1 | 5.1 | 22.40 | 20000 | 0.80 | 35 | 1984 | DD | 2 | 0.655 | 6389 |
| CFM Int'l | CFM56-3B2 | 5.1 | 24.30 | 22000 | 0.80 | 35 | 1984 | DD | 2 | 0.655 | 6607 |
| CFM Int'l | CFM56-3C1 | 5.1 | 25.50 | 23500 | 0.80 | 35 | 1986 | DD | 2 | 0.667 | 6766 |
| CFM Int'l | CFM56-5A1 | 6.0 | 26.60 | 25000 | 0.80 | 35 | 1987 | DD | 2 | 0.596 | 7770 |
| CFM Int'l | CFM56-5A3 | 6.0 | 27.90 | 26500 | 0.80 | 35 | 1990 | DD | 2 | 0.596 | 7850 |
| CFM Int'l | CFM56-5A4 | 6.0 | 23.80 | 22000 | 0.80 | 35 | 1996 | DD | 2 | 0.596 | 7375 |
| CFM Int'l | CFM56-5A5 | 6.0 | 25.10 | 23500 | 0.80 | 35 | 1996 | DD | 2 | 0.596 | 7534 |
| CFM Int'l | CFM56-5B1 | 5.7 | 30.20 | 30000 | 0.80 | 35 | 1994 | DD | 2 | 0.600 | 8366 |
| CFM Int'l | CFM56-5B2 | 5.6 | 31.30 | 31000 | 0.80 | 35 | 1993 | DD | 2 | 0.600 | 8479 |
| CFM Int'l | CFM56-5B3 | 5.4 | 32.60 | 33300 | 0.80 | 35 | 1997 | DD | 2 | 0.600 | 8734 |
| CFM Int'l | CFM56-5B4 | 5.9 | 27.10 | 27000 | 0.80 | 35 | 1994 | DD | 2 | 0.600 | 8036 |
| CFM Int'l | CFM56-5B5/P | 5.9 | 23.33 | 22000 | 0.80 | 35 | 1996 | DD | 2 | 0.600 | 7509 |
| CFM Int'l | CFM56-5B6/P | 6.0 | 24.64 | 23500 | 0.80 | 35 | 1995 | DD | 2 | 0.600 | 7659 |
| CFM Int'l | CFM56-5C2 | 6.8 | 28.80 | 31200 | 0.80 | 35 | 1991 | DD | 2 | 0.545 | 8796 |
| CFM Int'l | CFM56-5C3 | 6.7 | 29.90 | 32500 | 0.80 | 35 | 1994 | DD | 2 | 0.567 | 9122 |
| CFM Int'l | CFM56-5C4 | 6.6 | 31.15 | 34000 | 0.80 | 35 | 1994 | DD | 2 | 0.567 | 9285 |
| CFM Int'l | CFM56-7B20 | 5.4 | 22.61 | 20600 | 0.80 | 35 | 1996 | DD | 2 | 0.603 | 6963 |
| CFM Int'l | CFM56-7B22 | 5.3 | 24.41 | 22700 | 0.80 | 35 | 1996 | DD | 2 | 0.603 | 7194 |
| CFM Int'l | CFM56-7B24 | 5.2 | 25.78 | 24200 | 0.80 | 35 | 1996 | DD | 2 | 0.603 | 7360 |
| CFM Int'l | CFM56-7B26 | 5.1 | 27.61 | 26300 | 0.80 | 35 | 1996 | DD | 2 | 0.603 | 7602 |
| CFM Int'l | CFM56-7B27 | 5.0 | 28.63 | 27300 | 0.80 | 35 | 1996 | DD | 2 | 0.603 | 7872 |
| CFM Int'l | LEAP-1A26 | 11.1 | 33.40 | 27112 | 0.78 | 35 | 2015 | DD | 2 | 0.536 | 8840 |
| CFM Int'l | LEAP-1A35 | 10.7 | 38.60 | 32170 | 0.78 | 35 | 2015 | DD | 2 | 0.536 | 9401 |
| CFM Int'l | LEAP-1B25 | 8.4 | 38.40 | 26797 | 0.79 | 35 | 2016 | DD | 2 | 0.536 | 7778 |
| CFM Int'l | LEAP-1B27 | 8.5 | 39.90 | 28034 | 0.79 | 35 | 2016 | DD | 2 | 0.536 | 7898 |
| CFM Int'l | LEAP-1B28 | 8.6 | 41.50 | 29315 | 0.79 | 35 | 2016 | DD | 2 | 0.536 | 8024 |
| GE | CF6-6D | 5.9 | 24.70 | 40000 | 0.85 | 35 | 1970 | DD | 2 | 0.646 | 11749 |
| GE | CF6-6D1 | 5.9 | 24.70 | 41500 | 0.85 | 35 | 1971 | DD | 2 | 0.646 | 11895 |
| GE | CF6-6D1A | 5.9 | 25.40 | 41500 | 0.85 | 35 | 1971 | DD | 2 | 0.646 | 11895 |
| GE | CF6-45A2 | 4.3 | 25.90 | 46500 | 0.85 | 35 | 1973 | DD | 2 | 0.630 | 12927 |
| GE | CF6-50C | 4.3 | 28.80 | 51000 | 0.85 | 35 | 1975 | DD | 2 | 0.657 | 13323 |
| GE | CF6-50C1 | 4.3 | 29.80 | 52500 | 0.85 | 35 | 1975 | DD | 2 | 0.657 | 13467 |
| GE | CF6-50C2 | 4.3 | 28.44 | 52500 | 0.85 | 35 | 1978 | DD | 2 | 0.630 | 13467 |
| GE | CF6-50C2B | 4.3 | 29.06 | 54000 | 0.85 | 35 | 1979 | DD | 2 | 0.630 | 13611 |
| GE | CF6-50E | 4.3 | 28.44 | 52500 | 0.85 | 35 | 1973 | DD | 2 | 0.657 | 13505 |
| GE | CF6-50E2 | 4.3 | 29.80 | 52500 | 0.85 | 35 | 1973 | DD | 2 | 0.630 | 13505 |
| GE | CF6-80A | 5.0 | 29.00 | 48000 | 0.80 | 35 | 1981 | DD | 2 | 0.623 | 12883 |
| GE | CF6-80A2 | 5.0 | 30.10 | 50000 | 0.80 | 35 | 1981 | DD | 2 | 0.623 | 13076 |
| GE | CF6-80A3 | 5.0 | 30.10 | 50000 | 0.80 | 35 | 1981 | DD | 2 | 0.623 | 13069 |
| GE | CF6-80C2A1 | 5.1 | 30.96 | 59000 | 0.80 | 35 | 1985 | DD | 2 | 0.576 | 14782 |
| GE | CF6-80C2A2 | 5.1 | 28.00 | 52460 | 0.80 | 35 | 1986 | DD | 2 | 0.578 | 14034 |
| GE | CF6-80C2A3 | 5.1 | 31.64 | 58950 | 0.80 | 35 | 1988 | DD | 2 | 0.576 | 14776 |
| GE | CF6-80C2A5 | 5.1 | 31.58 | 60100 | 0.80 | 35 | 1988 | DD | 2 | 0.578 | 14907 |
| GE | CF6-80C2A8 | 5.1 | 31.00 | 59000 | 0.80 | 35 | 1996 | DD | 2 | 0.602 | 14782 |
| GE | CF6-80C2B1 | 5.1 | 30.08 | 56700 | 0.80 | 35 | 1987 | DD | 2 | 0.576 | 14529 |
| GE | CF6-80C2B1F | 5.1 | 30.13 | 57160 | 0.80 | 35 | 1989 | DD | 2 | 0.564 | 14628 |
| GE | CF6-80C2B2 | 5.1 | 27.74 | 51590 | 0.80 | 35 | 1987 | DD | 2 | 0.576 | 14039 |
| GE | CF6-80C2B4 | 5.1 | 30.36 | 57180 | 0.80 | 35 | 1987 | DD | 2 | 0.590 | 14575 |
| GE | CF6-80C2B6 | 5.1 | 31.56 | 60070 | 0.80 | 35 | 1987 | DD | 2 | 0.602 | 14851 |
| GE | CF6-80E1A1 | 5.1 | 32.46 | 67500 | 0.80 | 35 | 1993 | DD | 2 | 0.562 | 14844 |
| GE | CF6-80E1A2 | 5.1 | 33.10 | 68240 | 0.80 | 35 | 1993 | DD | 2 | 0.562 | 14844 |
| GE | CF6-80E1A3 | 5.1 | 35.70 | 68520 | 0.80 | 35 | 2001 | DD | 2 | 0.562 | 14844 |
| GE | CF6-80E1A4 | 5.1 | 34.50 | 66870 | 0.80 | 35 | 1997 | DD | 2 | 0.562 | 14844 |
| GE | CF34-10A | 5.4 | 26.50 | 18290 | 0.74 | 37 | 2010 | DD | 2 | 0.650 | 5453 |
| GE | CF34-10E | 5.1 | 27.30 | 18820 | 0.74 | 37 | 2002 | DD | 2 | 0.665 | 5598 |
| GE | CF34-3A | 6.3 | 19.70 | 9220 | 0.74 | 37 | 1986 | DD | 2 | 0.704 | 2849 |
| GE | CF34-8C1 | 5.1 | 23.03 | 12670 | 0.74 | 37 | 1999 | DD | 2 | 0.664 | 3988 |
| GE | CF34-8C5 | 5.1 | 23.09 | 13358 | 0.74 | 37 | 2002 | DD | 2 | 0.680 | 3935 |
| GE | CF34-8E5A2 | 5.1 | 24.82 | 14500 | 0.74 | 37 | 2002 | DD | 2 | 0.680 | 4129 |
| GE | GE90-76B | 8.6 | 35.45 | 79654 | 0.80 | 35 | 1995 | DD | 2 | 0.545 | 20930 |

System type: DD = direct-drive system

G = geared system

Appendix A (cont'd)

Engine database

| Org. | Engine Model | Thrust, lbs | | Cruise | Cruise Alt. | Year | System | No. of | Cruise TSFC | Propulsion System | |
|-------------|----------------|-------------|-----------|--------|-------------|-------|-----------|--------|-------------|-------------------|-------------|
| | | BPR (SLS) | OPR (SLS) | (SLS) | Mach | k ft. | certified | Type | Spools | lb/lb.hr | Weight, lbs |
| GE | GE90-85B | 8.4 | 38.37 | 87315 | 0.80 | 35 | 1995 | DD | 2 | 0.553 | 21656 |
| GE | GE90-90B | 8.4 | 39.70 | 94000 | 0.80 | 35 | 1997 | DD | 2 | 0.545 | 22280 |
| GE | GE90-94B | 8.3 | 40.53 | 97300 | 0.80 | 35 | 2000 | DD | 2 | 0.545 | 22592 |
| GE | GE90-115B | 7.1 | 42.24 | 115529 | 0.80 | 35 | 2003 | DD | 2 | 0.550 | 25876 |
| GE | GEnx-1B54 | 9.4 | 35.20 | 57394 | 0.85 | 40 | 2008 | DD | 2 | 0.514 | 16594 |
| GE | GEnx-1B58 | 9.2 | 37.20 | 60991 | 0.85 | 40 | 2008 | DD | 2 | 0.514 | 16952 |
| GE | GEnx-1B64 | 9.0 | 40.60 | 66993 | 0.85 | 40 | 2008 | DD | 2 | 0.514 | 17537 |
| GE | GEnx-1B70 | 8.8 | 43.50 | 72299 | 0.85 | 40 | 2008 | DD | 2 | 0.514 | 18054 |
| P&W | JT8D-7 | 1.1 | 15.82 | 14000 | 0.80 | 35 | 1966 | DD | 2 | 0.796 | 4508 |
| P&W | JT8D-9 | 1.0 | 15.88 | 14500 | 0.80 | 35 | 1967 | DD | 2 | 0.807 | 4646 |
| P&W | JT8D-17AR | 1.0 | 17.28 | 16400 | 0.80 | 35 | 1982 | DD | 2 | 0.825 | 4910 |
| P&W | JT8D-17R | 1.0 | 18.24 | 17400 | 0.80 | 35 | 1976 | DD | 2 | 0.825 | 5009 |
| P&W | JT8D-209 | 1.8 | 18.30 | 18500 | 0.80 | 35 | 1979 | DD | 2 | 0.724 | 5905 |
| P&W | JT8D-219 | 1.7 | 20.27 | 21000 | 0.80 | 35 | 1985 | DD | 2 | 0.737 | 6266 |
| P&W | JT9D-3A | 5.2 | 21.50 | 44300 | 0.85 | 35 | 1969 | DD | 2 | 0.624 | 12794 |
| P&W | JT9D-7 | 5.2 | 22.20 | 46300 | 0.85 | 35 | 1971 | DD | 2 | 0.620 | 13102 |
| P&W | JT9D-7A | 5.1 | 20.30 | 46950 | 0.85 | 35 | 1972 | DD | 2 | 0.625 | 13169 |
| P&W | JT9D-7F | 5.1 | 22.80 | 48000 | 0.85 | 35 | 1974 | DD | 2 | 0.631 | 13270 |
| P&W | JT9D-7J | 5.1 | 23.50 | 50000 | 0.85 | 35 | 1976 | DD | 2 | 0.631 | 13468 |
| P&W | JT9D-7Q | 4.9 | 24.50 | 53000 | 0.85 | 35 | 1978 | DD | 2 | 0.631 | 14055 |
| P&W | JT9D-7R4D | 5.0 | 23.40 | 48000 | 0.85 | 35 | 1978 | DD | 2 | 0.615 | 13553 |
| P&W | JT9D-7R4E | 5.0 | 24.20 | 50000 | 0.85 | 35 | 1982 | DD | 2 | 0.620 | 13565 |
| P&W | JT9D-7R4G2 | 4.8 | 26.30 | 54750 | 0.85 | 35 | 1982 | DD | 2 | 0.639 | 14220 |
| P&W | JT9D-7R4H1 | 4.8 | 26.70 | 56000 | 0.85 | 35 | 1982 | DD | 2 | 0.628 | 14340 |
| P&W | JT9D-20 | 5.2 | 20.30 | 46300 | 0.85 | 35 | 1972 | DD | 2 | 0.624 | 13097 |
| P&W | JT9D-70A | 4.9 | 24.50 | 53000 | 0.85 | 35 | 1974 | DD | 2 | 0.631 | 13990 |
| P&W | 1127G | 12.3 | 31.70 | 27000 | 0.78 | 35 | 2014 | G | 2 | 0.530 | 6300 |
| P&W | 1519G | 11.6 | 32.30 | 19000 | 0.78 | 35 | 2013 | G | 2 | 0.544 | 4800 |
| P&W | 2037 | 6.0 | 26.90 | 37600 | 0.80 | 35 | 1983 | DD | 2 | 0.563 | 10607 |
| P&W | 2040 | 5.5 | 29.40 | 40900 | 0.80 | 35 | 1987 | DD | 2 | 0.563 | 10972 |
| P&W | 2043 | 5.3 | 31.90 | 42600 | 0.80 | 35 | 1995 | DD | 2 | 0.563 | 11159 |
| P&W | 4052 | 5.0 | 26.32 | 52200 | 0.85 | 35 | 1987 | DD | 2 | 0.560 | 14027 |
| P&W | 4056 | 4.7 | 29.30 | 56750 | 0.85 | 35 | 1986 | DD | 2 | 0.560 | 14490 |
| P&W | 4060 | 4.5 | 32.40 | 60000 | 0.85 | 35 | 1988 | DD | 2 | 0.560 | 14819 |
| P&W | 4074 | 6.8 | 32.20 | 74500 | 0.85 | 35 | 1994 | DD | 2 | 0.560 | 19457 |
| P&W | 4077 | 6.7 | 33.20 | 77000 | 0.85 | 35 | 1994 | DD | 2 | 0.560 | 19950 |
| P&W | 4084 | 6.4 | 36.20 | 84000 | 0.85 | 35 | 1994 | DD | 2 | 0.560 | 20549 |
| P&W | 4090 | 6.1 | 39.16 | 90200 | 0.85 | 35 | 1996 | DD | 2 | 0.560 | 21522 |
| P&W | 4098 | 5.8 | 41.37 | 95340 | 0.85 | 35 | 1998 | DD | 2 | 0.560 | 22025 |
| P&W | 4152 | 4.9 | 26.90 | 52200 | 0.85 | 35 | 1986 | DD | 2 | 0.560 | 14036 |
| P&W | 4156 | 4.7 | 29.30 | 56750 | 0.85 | 35 | 1986 | DD | 2 | 0.560 | 14490 |
| P&W | 4164 | 5.2 | 31.24 | 64000 | 0.85 | 35 | 1993 | DD | 2 | 0.560 | 16886 |
| P&W | 4168-1D | 4.9 | 33.10 | 68600 | 0.85 | 35 | 2008 | DD | 2 | 0.560 | 17345 |
| P&W | 4460 | 4.7 | 30.68 | 60000 | 0.85 | 35 | 1988 | DD | 2 | 0.560 | 14802 |
| P&W | 4462 | 4.6 | 31.91 | 63300 | 0.85 | 35 | 1992 | DD | 2 | 0.560 | 15126 |
| P&W | 6122A | 4.8 | 25.70 | 22100 | 0.80 | 35 | 2004 | DD | 2 | 0.540 | 6311 |
| Rolls-Royce | RB211-22B | 4.7 | 25.00 | 41000 | 0.85 | 35 | 1973 | DD | 3 | 0.655 | 12098 |
| Rolls-Royce | RB211-524B | 4.5 | 28.40 | 49100 | 0.85 | 35 | 1973 | DD | 3 | 0.633 | 13270 |
| Rolls-Royce | RB211-524B4-02 | 4.4 | 29.00 | 50000 | 0.85 | 35 | 1981 | DD | 3 | 0.603 | 13309 |
| Rolls-Royce | RB211-524C2 | 4.5 | 29.10 | 51500 | 0.85 | 35 | 1979 | DD | 3 | 0.656 | 13370 |
| Rolls-Royce | RB211-524D4 | 4.3 | 29.70 | 53000 | 0.85 | 35 | 1983 | DD | 3 | 0.631 | 13606 |
| Rolls-Royce | RB211-524G | 4.3 | 32.10 | 58000 | 0.85 | 35 | 1989 | DD | 3 | 0.582 | 14040 |
| Rolls-Royce | RB211-524H | 4.2 | 34.00 | 60600 | 0.85 | 35 | 1989 | DD | 3 | 0.572 | 14186 |
| Rolls-Royce | RB211-535C | 4.5 | 21.50 | 37400 | 0.80 | 35 | 1981 | DD | 3 | 0.646 | 10338 |
| Rolls-Royce | RB211-535E4 | 4.1 | 25.40 | 40100 | 0.80 | 35 | 1983 | DD | 3 | 0.598 | 10648 |
| Rolls-Royce | AE3007A | 5.2 | 18.08 | 7580 | 0.78 | 32 | 1997 | DD | 2 | 0.625 | 2332 |
| Rolls-Royce | BR710-A1-10 | 4.2 | 24.23 | 14750 | 0.80 | 35 | 1996 | DD | 2 | 0.630 | 4640 |
| Rolls-Royce | BR715-A1-30 | 4.7 | 28.98 | 18920 | 0.76 | 35 | 1998 | DD | 2 | 0.620 | 6155 |
| Rolls-Royce | BR715-C1-30 | 4.6 | 32.15 | 21430 | 0.76 | 35 | 1998 | DD | 2 | 0.620 | 6155 |
| Rolls-Royce | Trent 1000-A | 9.5 | 41.00 | 70000 | 0.85 | 35 | 2007 | DD | 3 | 0.506 | 18056 |
| Rolls-Royce | Trent 553-61 | 7.5 | 35.19 | 56620 | 0.82 | 35 | 2000 | DD | 3 | 0.539 | 14843 |

System type: DD = direct-drive system
G = geared system

Appendix A (cont'd)

Engine database

| Org. | Engine Model | Thrust, lbs | | Cruise | Cruise Alt. | Year | System | No. of | Cruise TSFC | Propulsion System | |
|-------------|--------------------------|-------------|-----------|--------|-------------|-------|-----------|--------|-------------|-------------------|-------------|
| | | BPR (SLS) | OPR (SLS) | (SLS) | Mach | k ft. | certified | Type | Spools | lb/lbf.hr | Weight, lbs |
| Rolls-Royce | Trent 556-61 | 7.5 | 36.70 | 56620 | 0.82 | 35 | 2000 | DD | 3 | 0.539 | 14843 |
| Rolls-Royce | Trent 7000-72 | 9.0 | 45.40 | 73700 | 0.85 | 35 | 2018 | DD | 3 | 0.506 | 18864 |
| Rolls-Royce | Trent 768 | 5.2 | 34.00 | 68400 | 0.82 | 35 | 1994 | DD | 3 | 0.565 | 16839 |
| Rolls-Royce | Trent 772 | 5.0 | 35.80 | 71100 | 0.82 | 35 | 1994 | DD | 3 | 0.565 | 17105 |
| Rolls-Royce | Trent 772B-60 | 4.9 | 36.80 | 72000 | 0.82 | 35 | 1998 | DD | 3 | 0.565 | 17215 |
| Rolls-Royce | Trent 875 | 6.1 | 35.42 | 79100 | 0.83 | 35 | 1995 | DD | 3 | 0.560 | 19430 |
| Rolls-Royce | Trent 877 | 6.0 | 36.30 | 81300 | 0.83 | 35 | 1995 | DD | 3 | 0.560 | 19650 |
| Rolls-Royce | Trent 884 | 5.9 | 38.96 | 87700 | 0.83 | 35 | 1995 | DD | 3 | 0.560 | 20284 |
| Rolls-Royce | Trent 890-17 | 6.2 | 40.70 | 91300 | 0.83 | 35 | 1995 | DD | 3 | 0.560 | 20602 |
| Rolls-Royce | Trent 892 | 5.7 | 41.38 | 92500 | 0.83 | 35 | 1997 | DD | 3 | 0.560 | 20762 |
| Rolls-Royce | Trent 895 | 5.7 | 41.52 | 92900 | 0.83 | 35 | 1999 | DD | 3 | 0.560 | 20801 |
| Rolls-Royce | Trent 970-84 | 8.5 | 38.00 | 76100 | 0.85 | 35 | 2006 | DD | 3 | 0.518 | 19379 |
| Rolls-Royce | Trent XWB-84 | 9.0 | 41.10 | 85200 | 0.85 | 35 | 2013 | DD | 3 | 0.488 | 21163 |
| Rolls-Royce | Trent XWB-97 | 8.0 | 48.60 | 98200 | 0.85 | 35 | 2017 | DD | 3 | 0.488 | 22771 |
| IAE | V2500-A1 | 5.3 | 29.80 | 25000 | 0.80 | 35 | 1988 | DD | 2 | 0.580 | 7300 |
| IAE | V2522-A5 | 4.9 | 25.70 | 23043 | 0.80 | 35 | 1996 | DD | 2 | 0.575 | 7500 |
| IAE | V2524-A5 | 4.8 | 26.90 | 24518 | 0.80 | 35 | 1996 | DD | 2 | 0.575 | 7597 |
| IAE | V2525-D5 | 4.8 | 27.20 | 25000 | 0.80 | 35 | 1992 | DD | 2 | 0.575 | 7900 |
| IAE | V2527-A5 | 4.8 | 27.20 | 25000 | 0.80 | 35 | 1992 | DD | 2 | 0.575 | 7651 |
| IAE | V2528-D5 | 4.7 | 30.00 | 28000 | 0.80 | 35 | 1992 | DD | 2 | 0.575 | 8140 |
| IAE | V2530-A5 | 4.6 | 32.00 | 29900 | 0.80 | 35 | 1992 | DD | 2 | 0.575 | 8219 |
| IAE | V2533-A5 | 4.5 | 33.44 | 31600 | 0.80 | 35 | 1996 | DD | 2 | 0.575 | 8420 |
| NASA SFW | UH8 | 18.8 | 44.7 | 36833 | 0.80 | 35 | 2015 | G | 2 | 0.477 | 9300 |
| NASA AATT | N3CC-2016 | 17.6 | 31.6 | 18830 | 0.70 | 35 | 2040 | G | 2 | 0.461 | 5343 |
| NASA AATT | N3CC-2017 | 17.3 | 36.9 | 21515 | 0.78 | 35 | 2040 | G | 2 | 0.485 | 6012 |
| NASA AATT | N+3 | 27.5 | 36.6 | 28620 | 0.80 | 35 | 2040 | G | 2 | 0.464 | 9354 |
| NASA AATT | Small Core geared | 25.5 | 38.8 | 37659 | 0.80 | 35 | 2040 | G | 2 | 0.460 | 12152 |
| NASA AATT | N3CC-2018 | 21.6 | 36.7 | 21662 | 0.79 | 37.7 | 2040 | G | 2 | 0.479 | 6007 |
| NASA ERA | Large-DD-2015 | 16.6 | 43.7 | 71792 | 0.80 | 35 | 2030 | DD | 2 | 0.480 | 21399 |
| NASA ERA | Large-DD-2015-HWB-V1 | 14.4 | 48.9 | 67183 | 0.80 | 35 | 2030 | DD | 2 | 0.485 | 18768 |
| NASA ERA | Large-DD-2015-HWB-V2 | 13.7 | 49.8 | 67233 | 0.80 | 35 | 2030 | DD | 2 | 0.487 | 18832 |
| NASA ERA | Large-Geared-2015-HWB-V3 | 20.0 | 47.2 | 56172 | 0.80 | 35 | 2030 | G | 2 | 0.465 | 15591 |
| NASA ERA | Large-Geared-2015-HWB-V2 | 20.0 | 47.1 | 67423 | 0.80 | 35 | 2030 | G | 2 | 0.464 | 18823 |
| NASA ERA | Large-Geared-2015-HWB | 19.3 | 47.2 | 67386 | 0.80 | 35 | 2030 | G | 2 | 0.466 | 18823 |
| NASA ERA | Large-Geared-2015 | 24.7 | 39.9 | 74149 | 0.80 | 35 | 2030 | G | 2 | 0.458 | 23023 |
| NASA ERA | Medium-Geared-2015 | 23.9 | 38.4 | 45829 | 0.80 | 35 | 2030 | G | 2 | 0.466 | 13631 |
| NASA ERA | Medium-Geared-2015-V2 | 24.8 | 38.5 | 45799 | 0.80 | 35 | 2030 | G | 2 | 0.465 | 13668 |
| NASA ERA | Small-DD-2015 | 9.9 | 28.7 | 14647 | 0.80 | 35 | 2030 | DD | 2 | 0.526 | 3815 |
| NASA ERA | Small-DD-2015-V2 | 10.0 | 28.7 | 14686 | 0.80 | 35 | 2030 | DD | 2 | 0.525 | 3812 |
| NASA ERA | Small-Geared-2015 | 27.0 | 24.6 | 21525 | 0.80 | 35 | 2030 | G | 2 | 0.485 | 6203 |
| NASA ERA | Small-Geared-2015-V2 | 27.4 | 24.8 | 21553 | 0.80 | 35 | 2030 | G | 2 | 0.483 | 6232 |
| NASA ERA | Large-DD-2014 | 16.2 | 47.4 | 80071 | 0.80 | 35 | 2030 | DD | 2 | 0.469 | 22534 |
| NASA ERA | Large-Geared-2014 | 22.4 | 47.2 | 87496 | 0.80 | 35 | 2030 | G | 2 | 0.458 | 23248 |
| NASA ERA | Medium-Geared-2014 | 22.4 | 44.7 | 51295 | 0.80 | 35 | 2030 | G | 2 | 0.467 | 12645 |
| NASA ERA | Small-DD-2014 | 9.8 | 29.7 | 15566 | 0.80 | 35 | 2030 | DD | 2 | 0.519 | 3833 |
| NASA ERA | Small-Geared-2014 | 24.7 | 29.2 | 24887 | 0.80 | 35 | 2030 | G | 2 | 0.486 | 5913 |
| NASA SFW | SA-FPR1.4-DD-2D | 18.4 | 33.1 | 23813 | 0.80 | 35 | 2025 | DD | 2 | 0.479 | 10563 |
| NASA SFW | SA-FPR1.5-DD-2D | 15.0 | 33.8 | 23370 | 0.80 | 35 | 2025 | DD | 2 | 0.496 | 7965 |
| NASA SFW | SA-FPR1.6-DD-2D | 12.7 | 34.4 | 23046 | 0.80 | 35 | 2025 | DD | 2 | 0.510 | 6592 |
| NASA SFW | SA-FPR1.7-DD-2D | 10.9 | 35 | 22734 | 0.80 | 35 | 2025 | DD | 2 | 0.525 | 6099 |
| NASA SFW | SA-FPR1.3-GR-HW-2D | 24.1 | 32.6 | 26343 | 0.80 | 35 | 2025 | G | 2 | 0.470 | 8736 |
| NASA SFW | SA-FPR1.4-GR-HW-2D | 17.5 | 33.8 | 24917 | 0.80 | 35 | 2025 | G | 2 | 0.486 | 7401 |
| NASA SFW | SA-FPR1.5-GR-HW-2D | 14.6 | 33.5 | 23369 | 0.80 | 35 | 2025 | G | 2 | 0.502 | 6626 |
| NASA SFW | SA-FPR1.6-GR-HW-2D | 12.4 | 34 | 22924 | 0.80 | 35 | 2025 | G | 2 | 0.517 | 6252 |
| NASA SFW | SA-FPR1.3-GR-HW-2E | 26.0 | 32.3 | 28358 | 0.80 | 35 | 2025 | G | 2 | 0.473 | 8550 |
| NASA SFW | SA-FPR1.4-GR-HW-2E | 18.0 | 33.8 | 26575 | 0.80 | 35 | 2025 | G | 2 | 0.495 | 7123 |
| NASA SFW | SA-FPR1.5-GR-HW-2E | 12.1 | 35.4 | 24686 | 0.80 | 35 | 2025 | G | 2 | 0.515 | 6305 |
| NASA SFW | SA-FPR1.6-GR-HW-2E | 9.9 | 36.3 | 24262 | 0.80 | 35 | 2025 | G | 2 | 0.534 | 5896 |
| NASA SFW | SA-FPR1.7-DD-LW-2E | 8.5 | 37.6 | 23889 | 0.80 | 35 | 2025 | DD | 2 | 0.547 | 5561 |
| NASA SFW | Simulated Genx | 9.2 | 41.4 | 63800 | 0.85 | 35 | 2008 | DD | 2 | 0.523 | 17198 |
| NASA SFW | Simulated GE90-110B | 7.2 | 42 | 110000 | 0.85 | 35 | 2003 | DD | 2 | 0.549 | 23728 |

System type: DD = direct-drive system
G = geared system

SFW – Subsonic Fixed Wing project
ERA – Environmentally Responsible Aviation project
AATT – Advanced Air Transport Technology project